YARDANG AND DUNE CLASSIFICATION ON TITAN THROUGH LENGTH, WIDTH AND SINUOSITY.

D. Northrup[1], J. Radebaugh[1], E.H. Christiansen[1], S. Tass[1], L. Kerber[2] [1]Brigham Young University, S-389 ESC, Provo, UT USA 84602, [2]Jet Propulsion Laboratory, Pasadena, CA. northrup.dustin@gmail.com

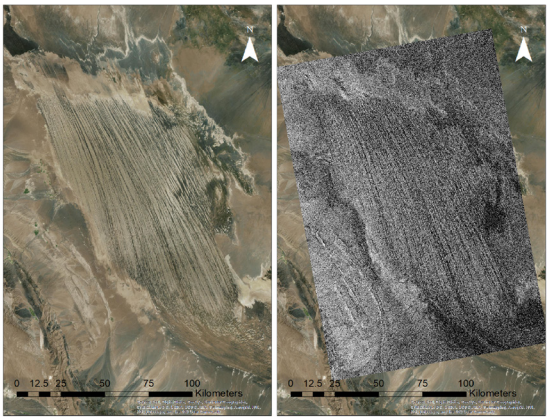

Fig 1. *(Left) Satellite image of yardangs in the Lut Desert of Iran. (Right) Radar image of yardangs in the Lut Desert of Iran with a resolution of ~300 m/pixel and 25% noise added.*

Introduction: Relatively straight, elongate ridges that form as wind erodes sediment and rock are known as yardangs (Fig. 1). These can be found in many deserts on Earth [1], Mars [2,3,4], and perhaps Venus [5] and Titan [6]. Generally forming in soft sediments such as lakebed clays [7] and volcanic ash [8], these features can form in resistant layers as well [9]. Yardangs typically form in regions characterized by arid conditions, lack of vegetation, and a persistent, unidirectional wind [1].

We describe general morphologies of yardangs in China, Argentina, Iran, and dunes and radar-bright features, potential yardangs, found in the northern midlatitudeds of Titan. We also seek to determine if yardangs can be distinguished from other features such as dunes based on statistical analyses of morphological parameters.

Western China Yardangs: We studied mesoyardangs in the Dunhuang Yardang field of western China. Erodable lakebed sediments at 40°30' N, 93°06' E form a series of discontinuous, highly parallel, and generally straight linear features [1, 11]. The yardangs display blunt upwind margins with streamlining downwind around the steep hills; they are up to 40 m high and generally discontinuous.

Argentinian Puna Yardangs: We studied yardangs in two separate fields in the Puna high plateau of NW Argentina. Characterized as hyperarid with prevailing NW-SE winds, the region has NW-SE oriented mega- and mesoyardangs form in ignimbrites located at 25°39'S, 66°47'W, and 26°36'S, 67°28'W respectively [8, 12, 13]. Megayardangs are significantly larger (>1 km) and appear to be typically found in more -consolidated materials than the mesoyardangs (<1 km) [8, 13, 14].

Both yardang types in Argentina display a blunt morphology on the upwind margin with a streamlined form on the downwind margin. The mesoyardangs display a more discontinuous morphology than the megayardangs and are more closely spaced.

Lut Desert Yardangs, Iran: Located at 30°09'N and 57°41'E, the yardangs found in the Lut Desert are formed in the 135 to 200 m thick Lut Formation which is composed of Pleistocene basin fill deposits [1, 14, 15] (Fig.1). The yardangs trend NW to SE with ridges attaining heights up to 80 m [1,15]. The individual ridges that form the entire measured yardang are significantly more closely spaced than in China or in the mesoyardangs of Argentina and are more sinuous other fields.

Features on Titan: Yardang-like features on Titan are found in the northern midlatitudes, in the T18, T23, T30, T56, T64, and T83 Cassini SAR swaths (Fig. 1). Though image resolution (~300 m) is much lower for Titan than satellite imagery of yardangs on Earth, the features differ from other regularly-spaced forms such as dunes in that they are SAR bright and appear less sinuous [6]. They are generally aligned NW to SE and are highly parallel, as is observed in the Earth yardang fields.

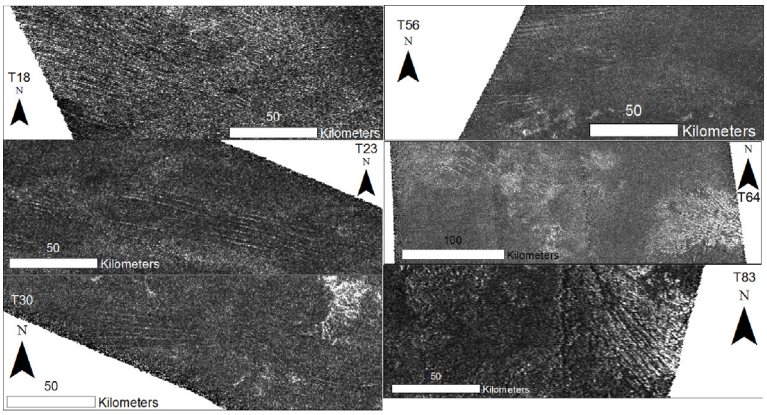

Fig 2. *Images of radar bright, linear features found in Titan SAR swaths T18, T23, T30, T56, T64, and T83.*

The features in T18 are densily populated and all share similar orientations (Fig. 2). No branching is visible. The features seen in swaths T23 and T30 appear to branch like dunes. Features in T64 show no branching and have a slight radial orientation, as sitting atop an elevated form [16] (Fig. 2). Features in T83 are similar to features in T64 but are less prominent and appear more weathered (Fig. 2). Features range in length between 4.5 km and 70 km, in width between 400 m and 1.3 km, in spacing between 700 m and 13 km, and sinuosity between 1 and

1.04.

Some linear features that are established as dunes, being SAR-dark and part of larger dune fields at low latitudes, are included in this study for comparison. These are from the T3 swath. They range in length between 10 km and 52 km, in width between 645 m and 1.3 km, in spacing between 1 km and 4.4 km, and sinuosity between 1.01 and 1.05.

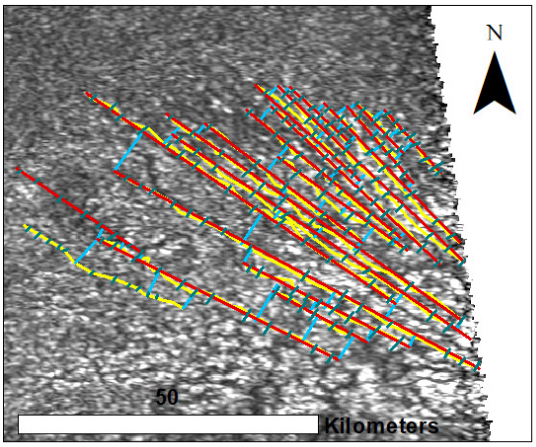

Fig 3. *SAR bright features seen in Titan swath T64. The red lines denote straight length, the yellow denote crest length. Width and spacing are denoted by the green and blue lines respectively.*

Feature Measurement Methods: Measurements of the yardangs were made using images acquired from ESRI World Imagery using IKONOS, with image resolution ~1 m [17]. Yardang crest length was measured as a line, not necessarily straight, down the center of each yardang. Width was obtained as straight lines across the yardang at regular intervals and then averaged down the yardang length. Yardang spacing was obtained by measuring from crest to crest of the adjacent yardang at regular intervals, averaged (Fig. 3). Sinuosity was obtained by dividing the crest length by the straight length.

Models: Statistical models were developed by predicting missing spacing data using a linear regression model with a multiple R^2 value of 0.71. The total yardang and dune data sets were then divided into training and test data sets. The initial training data set contained 301 terrestrial yardangs and 26 dunes (6 terrestrial and 20 titanian) selected at random. The measured Titan dunes are SAR dark and considered to be agreed upon as dunes. The test data set contained 300 terrestrial yardangs and 28 dunes (14 terrestrial and 14 titanian). A random forest, an ensemble learning method for classification and regression, was run on the training dataset to create a model to predict dune/yardang classification. Two models were developed, both of which gave the same predictions on the test data set with an overall classification rate of 98.8%, a correct yardang classification rate of 99.7%, and a correct dune classification rate of 89.3%. Model 1 classification parameters consisted of crest length, straight length, width, spacing, the ratio of width to spacing, sinuosity, the ratio of crest length to straight length, and the ratio of crest length. Model 2 used these same parameters with the inclusion of location. A third model was subsequently created using only terrestrial data as a training set. This model was then applied to all data from Titan with a 79% correct classification rate for dunes on Titan.

Discussion: The Model 1 (with terrestrial and titanian data) classified features as yardangs in SAR swaths T18, T23, T30, T56, and T64 with the highest number of classified yardangs being in T64. The second model classified features as yardangs in swaths T18 and T64 with T64 having the highest number of classified yardangs but it found no yardangs in T23, T30 and T83. The third model based only on terrestrial data classified some features as yardangs in all swaths. The Titan SAR swaths with the highest number of features classified as yardangs were T18, T30, and T64.

By coupling these models with detailed morphology observations and measurements it is possible to broadly distinguish between yardangs and dunes. When compared with measurements and observed morphologies in both terrestrial and titanian datasets the second model most accurately classifies features on Titan. Features in T18 appear very similar to radar images of yardangs in Iran's lut desert and features in T64 morphologically most closely resemble yardangs in Iran (Fig. 1&2). Features in T56 appears lighter than regular dunes, but still have dune-like aspects, such as a clear SAR difference between dune and interdune (Fig. 2). While the features on T83 morphologicaly closely resemble the features in T64 and the yardangs in Iran, they are not classified as yardangs by model 2, neither were they readily classified as yardangs in models 1 and 3 (Fig. 1&2).

References: [1] Goudie A.S. (2007) *Geography Compass 1*, 65-81. [2] Ward A.W. (1979) *Jour Geophysics Res 84*, 8147-8166. [3] Zimbelman J. et al. (2010) *Icarus 205*, 198-210. [4] Kerber L. et al. (2011) *Icarus 216*, 212-220. [5] Greeley R. (1999) *Technical Report*, ASU. [6] Paillou et al., Icarus (2015) Icarus. [7] Bristow C. et al. (2009) *Geomorphology* $_{105}$, 50-58. [8] de Silva S. et al. (2010) *PSS 58*, 459-471. [9] Elachi, C. et al. (2006) *Nature 441,709-713.* [10] Bridges N. et al. (2007) GRL. [11] Dong et al. (2012) *Geomorphology 139-140,* 145-154. [12] Inbar et al. (2001) *Earth Surface Processes and Landforms 26,* 657-666. [13] Halimov M., Fezer, F. (1989) *Zeitshcrift fur Geomorphologie 33, 205-217*. [14] Ehsani, A. et al. (2008) *Remote Sensing of Environment 112, 3284-3294.. [15] McCaulley et al. (1977) Geomorphology in Arid Regions, 233-269.* [16] Schurmeier et al. (2018) this meeting. [17] Dial, G., et al. (2003) *Remote Sensing of Environment 88, 23-36.*